Polarisation in High Resolution Radar Imaging

Shane R. Cloude, Julian M. Tealby,

Electronics Department, University of York,
Y01 5DD, England, UK

ABSTRACT

The use of polarisation in radar scattering and imaging has been studied by many authors and in this paper we review recent developments in the use of polarimetric tecniques in imaging for remote sensing applications. We consider two main applications, the use of optimum polarisation theory in polarimetric synthetic aperture radar (POLSAR) and the use of multi-polarisation imagery in ultra wide band (UWB) radar systems. We present results from analysis of SAR data and from a ground proibing radar system to support the techniques outlined.

INTRODUCTION

In this paper we review recent developments in the use of multiple wave polarisations for the construction and interpretation of radar images. We consier two main application areas; the exploitation of full scattering matrix information in Synthetic Aperture Radar (POLSAR) systems and the use of polarisation in time domain processing of ultra wide band (UWB) radars. The former are characterised by a low fractional bandwidth transmitted waveform and offer high spatial and range resolution (typically of a few meters) fully coherent scattering matrix data, which is used in remote sensing applications such as hydrology, forestry and sea ice monitoring [1]. The availability of such data has lead to interest in processing schemes which best utilise the full scattering matrix information. These techniues fall into two categories; the use of multiple transim/receive antenna polarisatiions for the generation of feature vectors for classification [2] and the use of optimum polarisation theory to maximise or minimise the return from specific target features of interest [3]. While the former are easier to implement, and have been successfully applied to remote sensing probems, the latter have been the subject of some controversy, particularly in the case of distributed targets such as vegetation and rough surface and volume scattering [4]. For this reason we concentrate on the latter and outine applications of the techniques to POLSAR data obtained from JPL SAR images. We use these results to outline potential difficulties with the interpretation of optimum polarisation data and suggest alternative processing techniques of use in the full exploitation of POLSAR image data.

The use of polarisation in ultra wide band (UWB) time domain radar imaging is a relatively new development and follows the empirical observation that linearly polarised time domain signals contain polarisation dependent information. We present experimental measurements from a remote sensing ground probing radar (GPR) to support this idea.

From these observations, we concude that the simultaneous measurement of co and cross linearly polarised signals can be used to generate correlations for the extraction of broad band signals form noise and the reconstruction of target geometry and shape. These UWB applications are distinguished from conventional microwave imaging by the use of ultra wide band signals, which not only have a large fractional transmitted bandwidth, but also contain frequency components which span the full range of target scale features. The received signals from such radars can be very complex, but by observation directly in the time domain, various canonical features of the target can be extracted using simple time gating tecniques.

While direct time domain measurements based on sampling technology are now possible with picosecond sampling resolution [5], the detection of such signals in noise poses new problems for receiver desing. In this case it is often advantageous to employ hybrid frequency/time signal processing, the general nature of which has recently been unified using the concepts of wavelets [6]. When combined with polarisation processing, this leads to a generalised concept of Huynen parameters [7] for target detection and identification. In this paper we consider one class of such processing techniques and use simulations to show how they may be used to improve detection of features in ground probing radar applications.

1. OPTIMUM POLARISATION THEORY FOR POLSAR SYSTEMS

There are two main classes of optimisation methods in radar polarimetry; single feature optimisation and statical target optimisation [4]. The two classes are distinguished by the type of target descriptor required. In the former the target is typically a localised scattering centre such as a specular surfaces or edge scattering return. In such cases target scattering is fully characterised by a 2 x 2 complex scattering matrix [S] [3]. For backscatter this matrix is symmetric and can be transformed into an arbitrary complex orthogonal base a unitary matrix transormation. It is well known that in one such base the matrix is diagonal [8] (note that this is true for any [S], the only constrain being that the matrix is complex symmetric). These two ortogonal polarisations are termed XPOL nulls as they represent a pair of *orthogonal* antenna polarisations for which the scattered wave has zero cross polar component. Together with a pair of copolar nulls (COPOL nulls), a pair of crosspolar maxima and two stationary phase points we arrive at a set of eight optimum polarisations for a general [S] matrix [8]. These polarisations are closely related to symmetry properties of the target and hience can be use for classification and identification of scattering centres. They have been investigated by many authors and in particular, when mapped on the Poincaré sphere, they form a geometrical construct known as the Polarisation Fork [9].

For example, the scattering matrix for backscatter from a small ellipsoidal particle is of the general form

$$[S] = \begin{bmatrix} \Delta \sin^2\delta \sin^2\theta + S_B & \Delta \sin^2\delta \sin\theta\cos\theta \\ \Delta \sin^2\delta \sin\theta\cos\theta & \Delta \sin^2\delta \cos^2\theta + S_B \end{bmatrix}$$

where θ is the canting angle of the particle, δ is a projection angle between the major axis and incident κ vector and $\Delta = (S_A - S_B)$ where S_A and S_B are the complex scattering coefficients for illumination parallel and perpendicular to the principal axes of the particle (these are functions of the permittivity and dimensions of the particle). This matrix be re-expressed in the form

$$[S] = \begin{bmatrix} \cos\theta & \sin\theta \\ -\sin\theta & \cos\theta \end{bmatrix} \begin{bmatrix} S_B & 0 \\ 0 & S_A\cos^2\delta + S_B\sin^2\delta \end{bmatrix} \begin{bmatrix} \cos\theta & -\sin\theta \\ \sin\theta & \cos\theta \end{bmatrix}$$

which shows how the canting angle determines the XPOL nulls (variation of the XPOL inclination angle can then be used to map variations in canting ange of the particle). The COPOL nulls are obtained from the ratio of eigenvalues of [S] and hence depend on the material properties and ellipticity of the particle [10]. Such an approach has been successfully applied to high resolution microwave images generated for canonical targets in a laboratory environment [11], but the study of natural targets requires and alternative approach to the optimisation problem to which we now turn.

The second class of optimisation theories apply to targets which require a stochastic description. Such classes arise often in SAR applications where, despite the fact that the resolution cell is only a few metres on side, it still contains a large number of scattering centres or a small number of centres which move over the finite time period required for measurement of the scattering matrix. In this case the individual [S] matrix measurements must be considered samples of a stochastic process and second order statics used to represent the target. Examples such as radar scattering from rough surfaces, vegetation, forestry and hydrometeors all fall into this category.

There are three main formulations of target scattering based on this stochastic model, the 4 x 4 real Mueller or Stokes refection matrix [M], the 4 x 4 Hermitian covariance matrix [C] and the 4 x 4 Hermitian Coherency matrix [T]. It is important to realise that in this case the optimisation procedure is more complicated, there being several more parameters available for optimisation and the matrix algebra involves 4 x 4 matrices in place of the 2 x 2 scattering matrix formulation. Cloude [4] has presented a classification of such procedure and here we concentrate on three important consequences of this analysis for the application of optimisation methods to radar images.

1.1 Target Decomposition and Optimisation Theory

Figure 1 (a) shows the copolar received power for backscatter form an ellipsoidal particle with $S_A = 3$, $S_B = 1$ and $= 30°$, plotted as a function of antenna polarisation ellipticity (Tau) and inclination angle (Theta). We see that there are maxima and minima as expected from the single feature theory. In contrast, figure 1 (b) shows the copolar power from a distributed target, in this case obtained from a JPL SAR image of San Francisco parkland using the POLTOOL software package. The Mueler matrix [M] and coherency matrix [T] for this target are given by

$$[M] = \begin{bmatrix} 1.000 & -0.1401 & 0.0477 & 0.0105 \\ -0.1401 & 0.5424 & 0.0165 & -0.0523 \\ 0.0477 & 0.0165 & 0.3685 & 0.0588 \\ 0.0105 & -0.0523 & 0.0588 & 0.0890 \end{bmatrix}$$

$$[T] = \begin{bmatrix} 0.4555 & -0.0701 + 0.0294\,i & 0.0239 + 0.0261\,i \\ -0.0701 - 0.0294\,i & 0.3157 & 0.0082 - 0.0052\,i \\ 0.0239 - 0.0261\,i & 0.0082 + 0.0052\,i & 0.2288 \end{bmatrix}$$

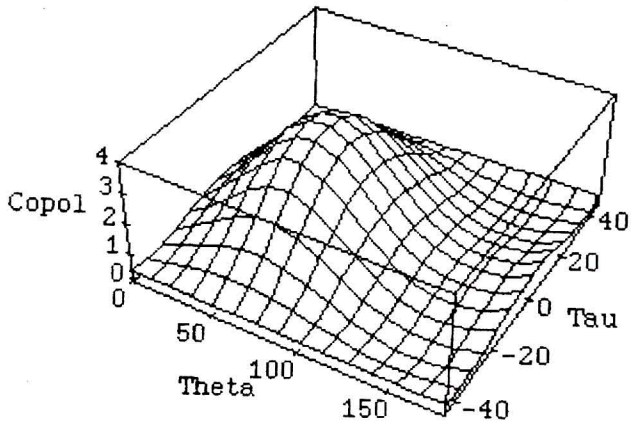

Fig. 1(a) - Copol power for ellipsoid at 30 degrees.

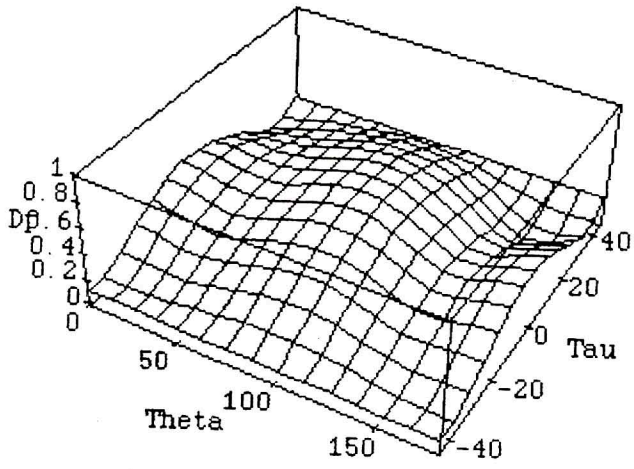

Fig. 2(a) - Degree of Polarisation of Copol Signal for SAR Image.

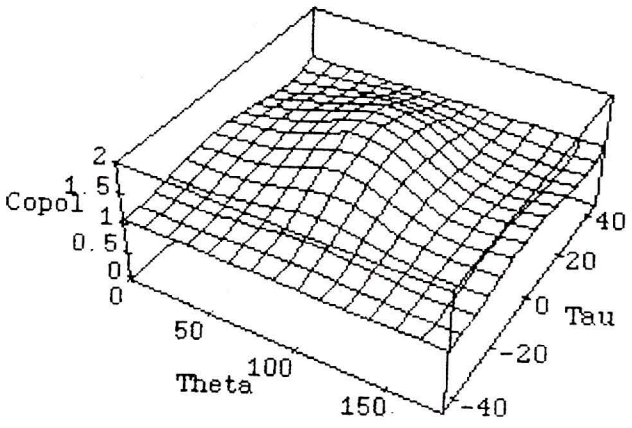

Fig. 1(b) - Copol power for SAR image of San Francisco Parkland.

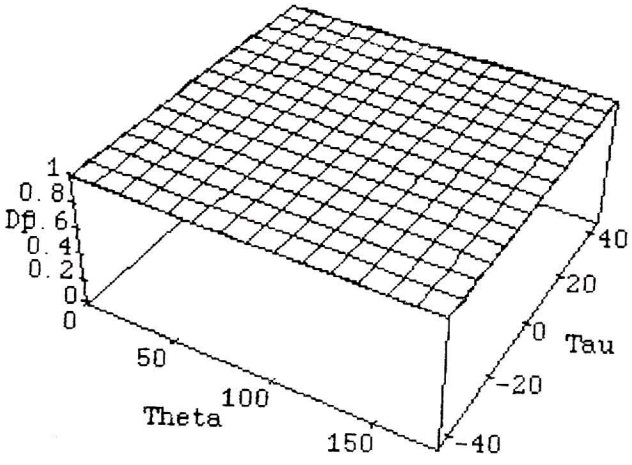

Fig. 2(b) - Degree of Polarisation for Copol Signal from Ellipsoid.

The coherency matrix has eigenvalues λ = (1, 0.580, 0.448) which displays the eigenvalue spectrum characteristic of a distributed target.

Many authors have studies such plots and noted the following general features [12]; although there are *local* maxima and minima, the nulls o not fall to zero for distributed targets. There appears a pedestal which bounds the minimum copolar signal power. Similarly, for distributed targets the degree of polarisation of the scattered wave depends on antenna polarisation. This is shown in figures 2 (a) and 2 (b) for the two targets considered above. Note that the degree of polarisation is constant for the ellipsoidal particle but varies with antenna polarisation for the distributed target. This has lead some authors to caste the optimisation problem in terms of the maximum degree of polarisation rather copolar power [13].

The above anaysis has lead to the suggestion that the copolar power variation might correspond to a single feature scattering matrix on top of a 'random' component represented by the pedestal. If this were the case then the single feature optimisation procedure could be applied to the 'equivalent target' so removing the need to consider a more general optimisation theory. This problem has been considere under the more general topic of target decomposition theorems as first developed by Huynen [14] and discussed at a recent NATO workshop on radar polarimetry [15]. In such theories we can represent a general target Ω as the noncoherent combination of up to four single matrix components; weighted by the eigenvalues of the target coherency matrix as [15]

$$\Omega = \sum_{i=1}^{4} \sqrt{\lambda_i}\,[S_i]$$

where the $[S_i]$ are obtained from the eigenvectors of the coherency matrix and λ_i are the corresponding eigenvalues.
The expression for copolar power may be expressed in terms of a 6th order polynomial in the complex polarisation ratio of the antenna [4] (similar polynomial expression may be derived for optimisation of the cross polar power or degree of polarisation signatures). It then follows from the target decomposition theorem that the coefficients of this polynomial are given by the weighted sum of contributions from each of the four targets. For this reason the optimum polarisation states do not correspond to those of the dominant target component (given by the eigenvector corresponding to the largest eigenvalue of the coherency matrix and this has two important implications for the interpretation of optimum polarisations for distributed targets:
a) The optimum polarisations for distributed targets are obtained from a combination of all four target components and hence are not clearly related to dominant scattering mechanisms in the target. Hence any interpretation of these states in terms of physical properties of the scattering volume is difficult. A better approach would be to extract the null states of the dominant eigenvector, as these are related to dominant scattering components, such as average canting angle for a cloud of ellipsoidal particles [16].

b) The extraction of a single scattering matrix plus noise plateau is not possible for the general optimisation process due to the possibility of four *distinct* eigenvalues for the coherency matrix. This means that in general, the copolar maxima will not be orthogonal, as they are for single feature optimisation, and that the Huynen fork the representation cannot be used for such targets. Thus the startegy of replacing a distributed target optimisation by a single feature plus noise pedestal is not generally possible.

1.2 Iterative Techniques and Polynomials in Optimisation

As discussed above, the optimisation process for distributed targets generates a 6th order polynomial equation for the unknown complex polarisation ratio. There are two main methods for finding the optimum states from this equation [4]. In the first we can use root searching algorithms to estimate the six complex roots. Alternatively we can use iterative techniques such as Newtons method to converge on the root given a suitably accurate initial estimate. The main problem with the former is that finding the roots of high order polynomials can be an ill-posed problem, with large errors occuring in the determination of the roots for small errors in the polynomial coefficients. The second technique employing iterative methods relies on good initial estimates for convergence. Such estimates can be provided by using the null states for the dominant eigenvector as discussed in [4].

1.3 Contrast Optimisation Algorithms

As an alternative to finding the optimum polarisation states for a target in isolation, several authors have suggested the alternative strategy of optimising the *contrast* between two targets as a more suitable parameter for applications in remote sensing. Initial work in this area was performed by Ioannidis and Hammers [17] using the Mueller matrix for two target classes. More recently however, there has been proposed a technique based on the target covariance matrices for the two targets [18]. In this method the optimum contrast states are generated from the eigenvectors of a matrix obtained as the product of the two class covariance matrices and the optimum contrast rarios are given by the corresponding eigenvalues. Unfortunately, this technique provides a bias to polarisation states on the Poincaré sphere [19] and hence is not guaranteed to provide optimum contrast, nor does it provide optimum states which bear any physical significance to the dominant scattering process. Such contrast algorithms must then be used with great care.
To illustrate the above features and reinforce their application to remote sensing, figures 3 (a) and (b) show copolar images obtained from JPL SAR data of Alcatraz island. In figure 4 (a) we choose a transmit polarisation which is a COPOL null for the dominant eigenvector of the coherency matrix of the ocean (obtained by *averaging* over a number of ocean pixels). This optimum polarisation state corresponds to the dominant specular reflection characteristic for returns from the ocean at high angles of incidence. Here we see very good contrast between the island and ocean. Figure 3 (b) on the other hand shows the same image obtained using the XPOL null for the sea return (again obtained from the dominant eigenvector). In this case we see much more detail of the ocean backscatter and can see features not apparent in the COPOL image. The maximum eigenvector method is successful in this case because the signals from the ocean are highly correlated and the covariance matrix has a clear dominant eigenvalue. Clearly we can use such processing to enhance features of interest in SAR images and to improve the contrast between target classes.

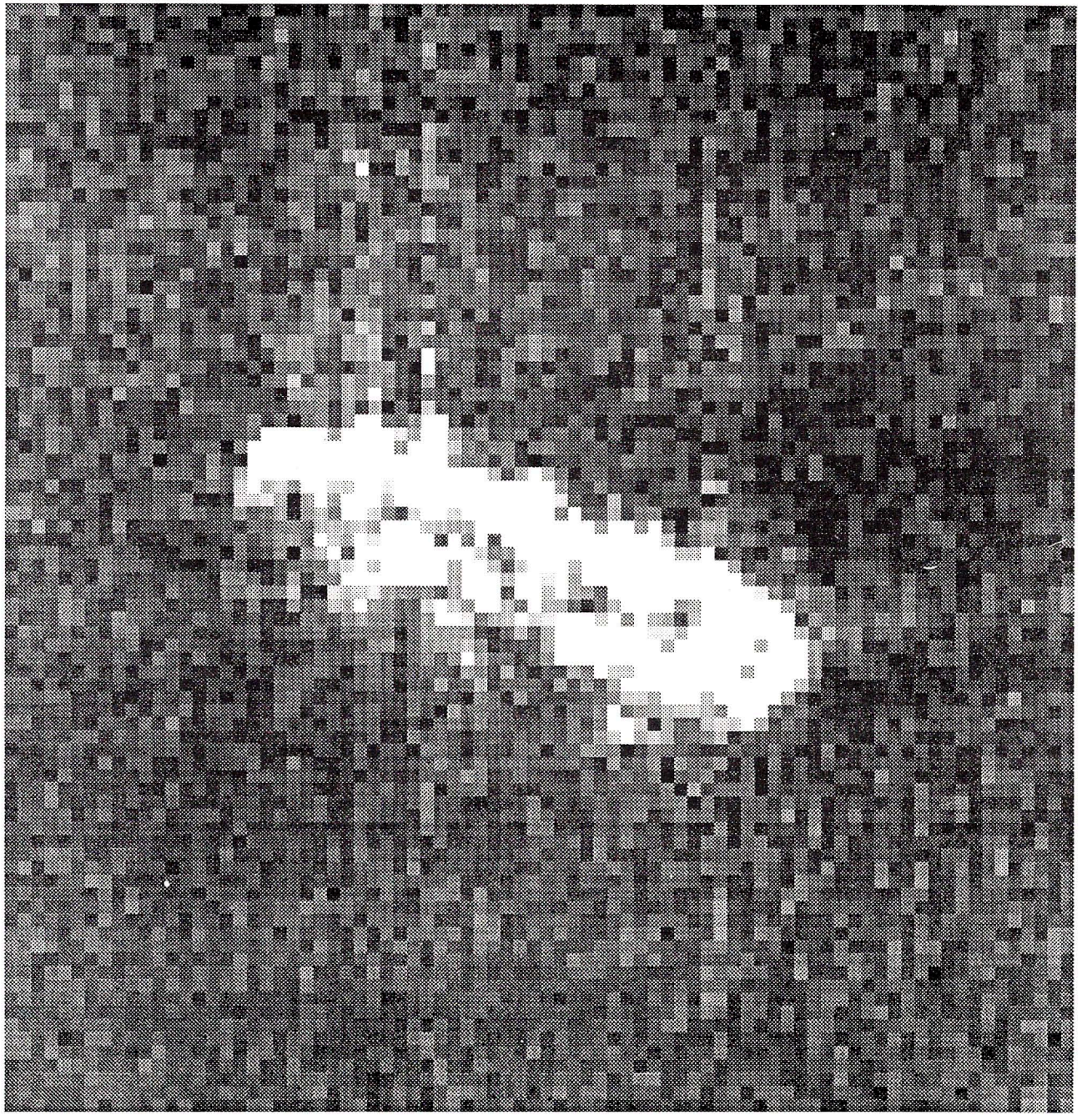

Fig. 3(a) - Copolarised SAR Image of Alcatraz Island usign COPOL Null of Maximum Eigenvector.

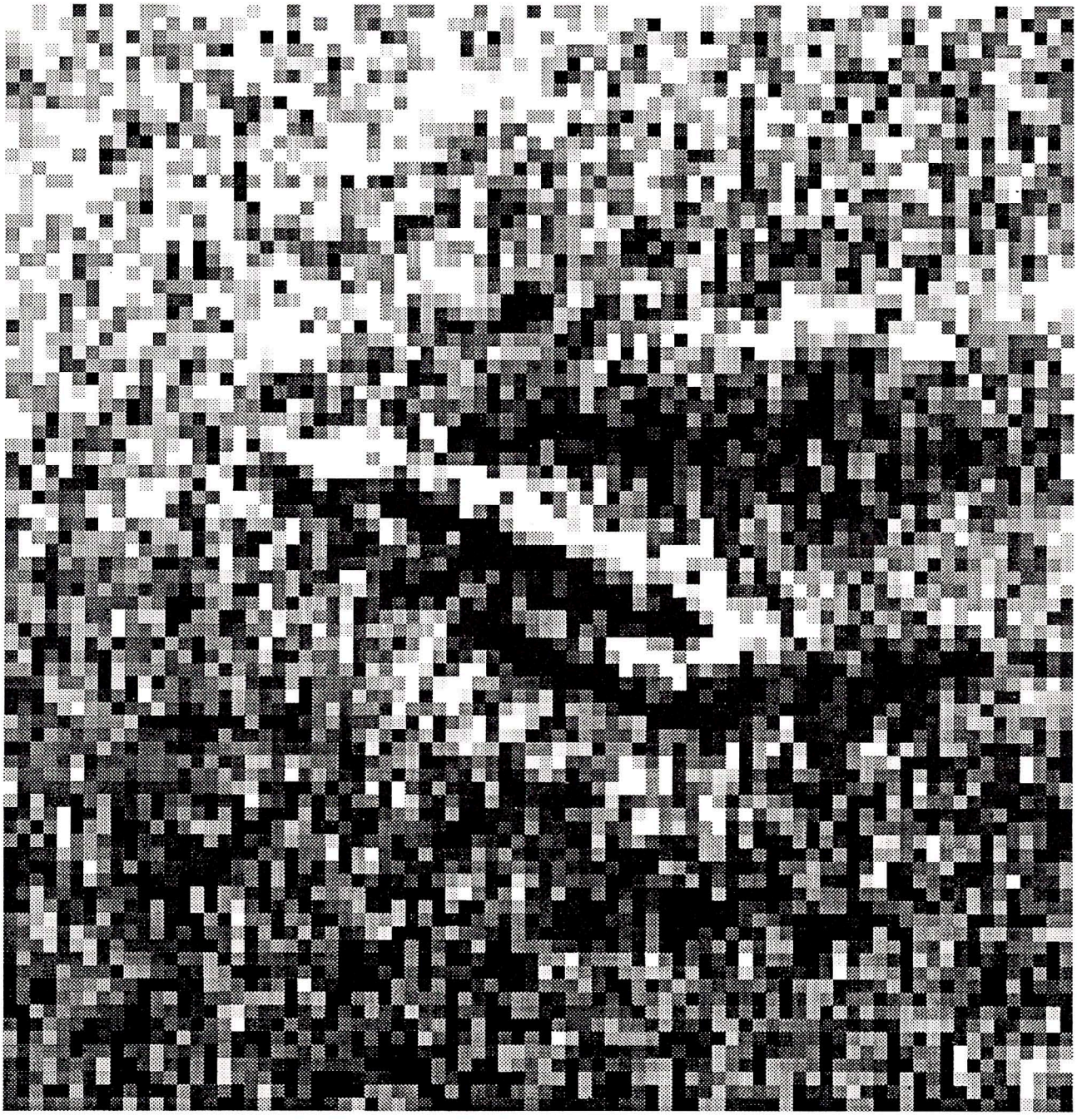

Fig. 3(b) - Copolarised SAR Image of Alcatraz Island using XPOL Null for Maximum Eigenvector.

2. PROPAGATION OPERATORS FOR SAR IMAGE ANALYSIS

Above we considered the application of optimum polarisation theory to SAR imaging. Here we consider a matrix differential calculus for analysing the *change* in polarisation behaviour of such images. This could be used to identify boundaries between different polarimetric targets in an image and for the classification of image texture based on complete scattering matrix information.

The classical calculus for determining changes in polarisation was developed by Jones for light propagation in crystals. This calculus is governed by a differential [N] matrix defined by [16].

$$\frac{d[S]}{dt} = [N][S] \qquad [N] = \begin{bmatrix} \alpha+\beta & \gamma - i\delta \\ \gamma + i\delta & \alpha - \beta \end{bmatrix}$$

where [N] is of the general form shown, for α, β, γ, and δ all complex. These parameters are interpreted as generalised wave propagation factors and hence describe the dynamic behaviour of the wave as it progresses through the medium.

This approach has been generalised, first to deal with the 4 x 4 Mueller calculus and most recently to the case of the coherency matrix [16]. Whereas for the Jones calculus there are 8 elementary types of dynamic behaviour governed by the complex numbers α, β, γ and δ, in the case of the coherency matrix there are potentially 16 different types of behaviour. However, by restricting attention to changes in the dominant eigenvector for backscatter only, it has been shown that there are 8 types of dynamic behaviour governed by the 8 Gell-Mann matrices from quantum mechanics [20]. For example, we can generate changes in target orientation angle by using the following basis matrix (Γ) and matrix exponential mapping

$$\Gamma = \begin{bmatrix} 0 & 0 & 0 \\ 0 & 0 & i \\ 0 & -i & 0 \end{bmatrix} \Rightarrow \exp(i\alpha\Gamma) = \begin{bmatrix} 1 & 0 & 0 \\ 0 & \cos\alpha & -\sin\alpha \\ 0 & \sin\alpha & \cos\alpha \end{bmatrix}$$

This can be used to analyse experimental scattering matrix data by projecting measured [S] values into the eigenvectors of propagation operators. Note that by doing this we can 'select' to view parameter variations across a field of view, even in the case of multiple parameter dependency.

To illustrate, consider the computer simulated SAR image shown in figure 4. Here we assume a stochastic target model which models the individual pixel matrices according to a statical distribution. We assume however that the pixels have a high degree of polarimetric coherence and contain a correlated pattern of preferred orientation such that the dominant eigenvectors of the pixel coherency matrix is of the form given for ellipsoidal particels.

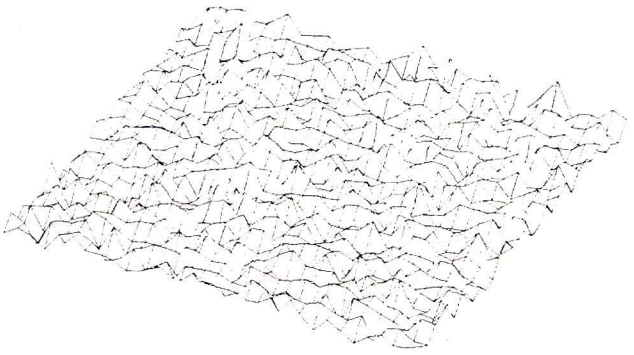

Fig. 4(a) - HH SAR Image of Oriented Scatterers with Random Perturbations.

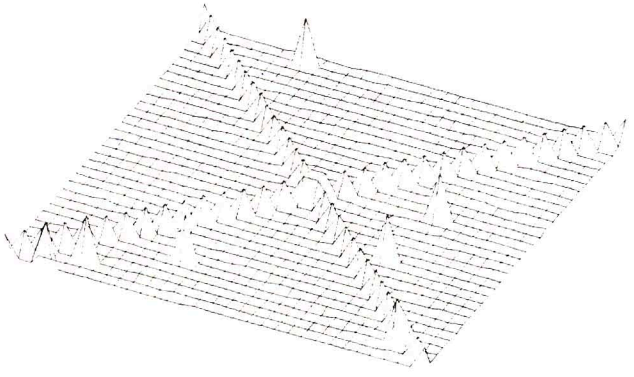

Fig. 4(b) - SAR image of Phase of Projection of [S] onto Rotation Eigenvector.

To illustrate multiple parameter dependance, we let δ, S_A and S_B vary randomly from pixel to pixel. The result for a synthesised HH scalar image is shown in figure 4 (a). Here we cannot detect the correlated orientation angles as they are masked by fluctuations caused by the other three parameters. However, by projecting the pixel matrices onto the eigenvectors of Γ, as given by the columns of the matrix [E] shown below, and forming an image from the phase of this projection we obtain the image shown in figure 4 (b).

$$[E] = \begin{bmatrix} 0 & 0 & 1 \\ i & 1 & 0 \\ 1 & i & 0 \end{bmatrix}$$

Note that we can now clearly see the spatial correlation of orientation angles hidden in the image, which in this simulation was pre-arranged in the form of a figure X.

This example shows how, by projecting [S] matrix data onto eigenvectors of propagation matrices such as Γ, we can examine spatial correlations not apparent in conventional scalar images.

The success of this method relies on nowledge of the eigenvectors of propagation matrices, all of which can be generated using group theoretical ideas borrowed from the quantum mechanics literature on Lie groups [20].

3. ULTRA WIDE BAND RADAR TECHNIQUES

In the last section we considered the use of polarisation information in SAR imaging. Here we consider how multi-polarisation imaging can be used in ultra wideband (UWB) radar techniques. Such radars are characterised by two important features: the effective bandwidth Δf of the transmitted waveform is large compared to the centre frequency f_C. We describe this fractional bandwidth by a parameter μ as shown below

$$\mu = \frac{\Delta f}{f_c}$$

For UWB applications we deal with waveforms for which $\mu > 1$.

Secondly, the scattering object has dimensions which represent widely different scales to the incident signal i.e. the object responds to low frequency, resonant and high frequency components in the incident wave. It is important to realise that all three components are excited simultaneously in UWB radar applications. For the purposes if imaging this is important since the low frequency information is used to image global structure of the object while the high frequencies offer fine detail on scattering centres. This is in marked contrast to conventional microwave imaging radars which provide only high frequency information on localised scattering centres. Note that while spatial image resolution is related to absolute bandwidth, UWB radars are characterised by a large fractional bandwidth μ.

The design of systems to employ such signals poses severe problems in three main categories: the generation of high transmitter power so that the signal to noise ratio in the receiver is adequate for band detection; the requirement for design of UWB antennas to faithfully transmit such signals and finally, the design of broad band receivers to detect weak signals against noise.

The first of these can be overcome by using a swept frequency source with pulse compression to simulate the effect of an UWB pulse. Alternative and simpler technology is emerging from the high pulse power community [21] and can be used to generate pulse waveforms directly.

The second problem of antenna design is more serious. It is fundamentally difficult to design directive broad band antennas with an effective impedance match across the band of an UWB radar. Consequenty most UWB systems employ one of only a few antenna designs: resistively loaded dipoles are commony employed but they are not directive and have power limitatioins. Other antennas include biconic antennas, TEM horns and fins. The problem of receiver design can be met by employing a conventional superheterodyne receiver combined with a swept frequency source, but the requirement for *coherent* measurements across a wide band leads to increased complexity, expense and long measurement times.

Alternative and simpler technology is now available for measurements directly in the time domain using fast sampling technology [5]. This can be based on repetitive sampling techniques which require a high PRF, or on single shot sampling systems, both of which can be used to make measurements on picosecond time scales. Such methods can be used to improve the signal to noise ratio through averaging and correlation techniques. The technology underlying UWB radar has recently been reviewed in a SPIE publication [21] and here we concentrate on two important topics: the use of hybrid time/frequency analysis for imaging based on UWB signals and the use of polarisation for UWB imaging.

4. ANALYTICAL TECHNIQUES FOR UWB RADARS

There are three main techniques used for a description of UWB waveforms. The concept of analytic signals used in quasi-monochromatic analysis can be extended to permit a complex representation of UWB signals, but the theory quickly becomes unwieldy and offers little insight into the mechanisms of UWB radar scattering. This is mainly because such waveforms are dominated by time discontinuities, the representation of which in the Fourier domain is difficult. Such models represent time signals in the form

$$A(t) \exp [\, i (\omega_c t + \varphi(t)) \,] = r(t) + i\, s(t)$$

where the signals r(t) and s(t) are related by a Hilibert Transform [22]. In many UWB applications however there is no clear concept of a carrier frequency ω_c modulated by an envelope as implicit in the analytical signal model. For these reasons such an approach is generally only useful for narrowband signals wen $\mu < 0.5$.

A second approach to modelling UWB signals is to use direct time domain techniques. Such analysis is based on direct time domain analysis of Maxwells equations and focusses on the characterisation of time discontinuities in the UWB signal. However, the treatment of polarisation in the time domain is difficult: it is easy to generalise the concept of orthogonal linear polarisations, but the generalisation of orthogonal elliptical states is difficult.

As an example of the use of direct time domain techniques, consider the well known Kennaugh-Cosgriff inverse scattering identity relating the backscattered impulse response of a target to its silhouette area function [23]. This approximation is based on physical optics and, for a sphere, leads to the impulse response approximation shown in figure 5(a). Note that there are two important time discontinuities

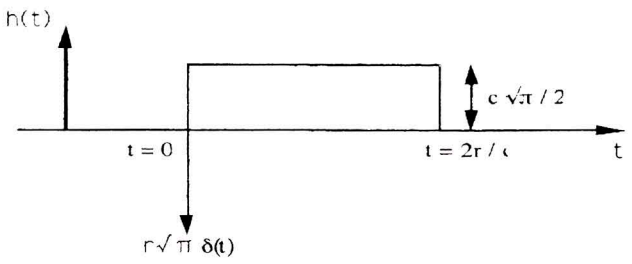

Fig. 5(a) - Physical Optics Impulse Response of Metallic Sphere radius r.

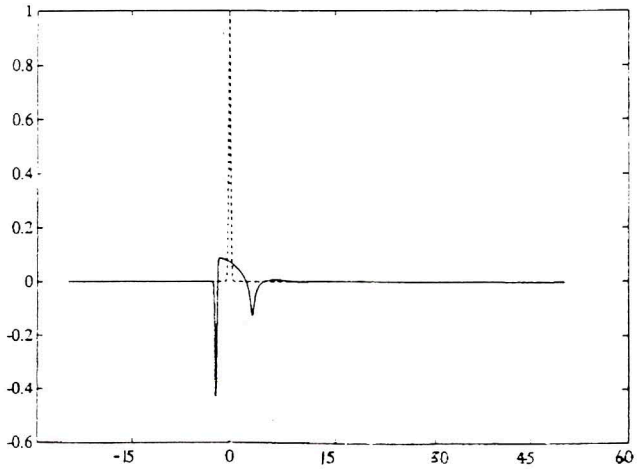

Fig. 5(b) - Impulse Response for Metallic Sphere from Mie Series Calculations.

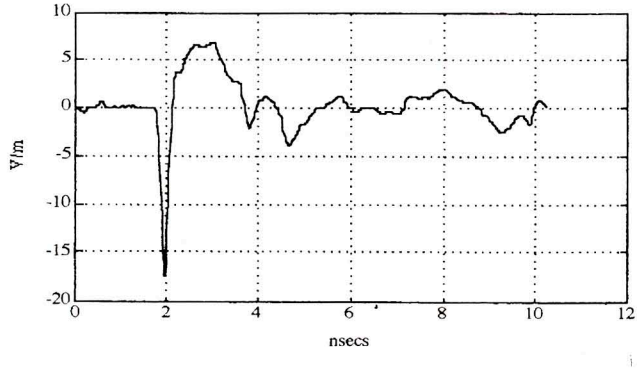

Fig. 5(c) - Measured Impulse Response for 30 cm Diameter Sphere.

which generate the form of this response, a geometrical optics specular return from the front of the sphere (which generates the delta function on the front edge of the response) and the shadow boundary assumed in physical optics which generates the sharp cutoff after 2r/c seconds. To extend this approximation, figure 5(b) shows the impulse response obtained from Fourier transform of Mie series data for the sphere. Note that the specular flash is present together with a second discontinuity, a creeping wave contribution not predicted by the physical optics approximation. Figure 5(c) shows the results of an experimental measurement of radar backscatter from a 30 cm diameter metallic sphere using a radiated impulse waveform of 120 ps duration. Note that the specular flash and creeping wave contributions are clearly visible, together with an artifact at round 4ns which is due to reflections from the sphere support. The advantage of time domain techniques is that we can identify such responses by direct inspection of the signal. The interpretation of these phenomena in the frequency domain is very difficult. Recently there has been much interest in the use of coherent states or wavelets for the representation of nonstationary transient waveforms [24]. Such analysis has been applied to seismic data and speech waveforms and has recently been proposed for application to UWB radar data [25]. In this case the advantages of transform techniques are combined with the resolution of discontinuities inherent in the time domain. This combination is provided by the use of basis functions which are localised both in the time and frequency domains, hence the concept of a wavelet (contrast this with the Fourier basis wich are of infinite extent in the time domain and localised only in the frequency domain). Such basis states can be generated from a 'mother' wavelet using group theoretical considerations of transformation under scale and translation. The two main classes of coherent states are those generated from the Weyl-Heisenberg group (which generates localised wave packets as basis functions) and wavelets, which are generated from the affine group of translations and scale change [26].

In this paper we consider the simpler class of Gabor waves for which the basis functions are one sided damped exponential waves [27]. In this representation we can express an arbitrary time waveform y(t) in the form

$$y(t) = \sum_{m,n=-\infty}^{\infty} C_{m,n}\, g(t - n\alpha) \exp[\, i\, 2\pi\, m\, \beta\, t\,]$$

where the C_{mn} are complex coefficients, g(t) is a window function and α represents a change in time scaling of the waveform (usually we assume $\alpha\,\beta = 1$). As an example of how such coefficients can be used in radar imaging, consider figure 6(a) which shows the measured UWB radar response of a ciruclar cylinder viewed end on and illuminated by an impulsive waveform of 120 ps width. Note that the front and rear of the cylinder are clearly located as nonstationary signals in the time domain response, Figure 6(b) shows the Gabor spectrum for this signals. Two components can clearly be identified with the front and rear of the cylinder. To see how such waves can be used in polarisation analysis of UWB signals, we now turn to consider polarisation measurements using a ground probing radar system based on UWB radar.

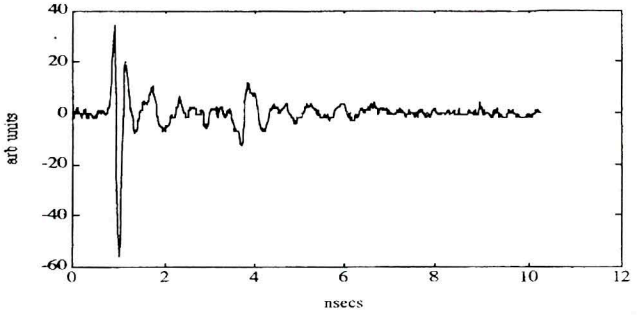

Fig. 6(a) - Measured Impulse Response for 40 cm Cylinder.

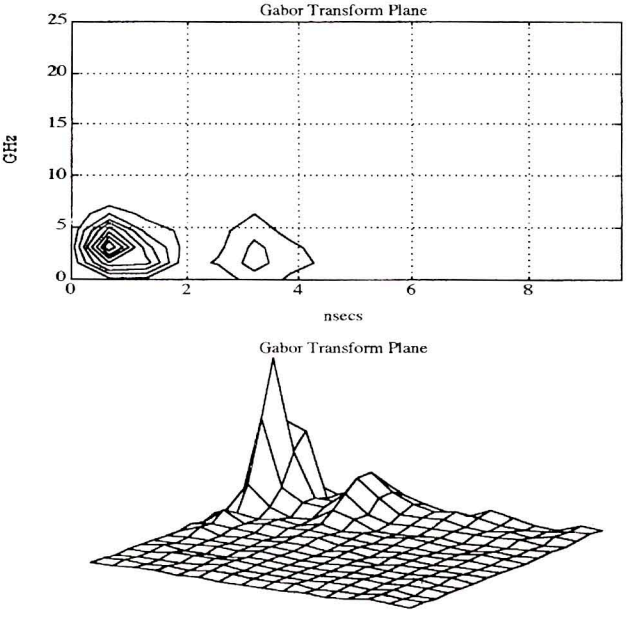

Fig. 6(b) - Gabor Transform of Cylinder Impulse Response.

5. APPLICATIONS OF POLARIMETRIC UWB RADAR TO REMOTE SENSING

One of the most important applications of UWB radar is in ground probing radar (GPR). Such systems have been used for military applications such as mine detection for many years but more recently there has been great interest in applying this technology to remote sensing applications such as archaeological surveying and hydrology. We have used such a system for investigating the interior structure of the mediaeval walls of York. The system uses a pulse source of approximately 1ns duration and a pair of resistively loaded dipole antennas for transmission and reception. The antennas can be made parallel or perpendicular to receive co or cross polarised time domain signals. By moving the radar over the surface, an image of subsurface features can be constructed. Figure 7 shows two such images for the York wall survey. In both cases the horizontal axis represents distance along the wall and the vertical axis is time. Note that the only pre-processing performed on these images is to filter the radar returns and apply a time dependent gain to compensate for attenuation in the material of the walls. The two images are for the same strech of wall but differ in the orientation of the receive antenna: in figure 7 (a) the receiver is oriented parallel to the transmitter while in figure 7 (b) the receiver is orthogonally polarised to the transmitter. Shown in the lower part of the figure is a schematic of the surveyed wall geometry. Note that the arch structure to the right of the image is clearly shown in both images. Importantly however, the two images contain different information. This was confirmed by combining the two signals to locate two voids in the wall, one of which is in the top left of the copolar image and the other in the centre of the cross polar image. These images illustrate the importance of polarisation information in UWB imaging.

Future studies will be centred around simultaneous synchronised measurement of both co and cross polarised signals. This will permit comparison of time shifts between co and cross polarised signals which may be used to further enhance the identification of structure in these images and to detect objects against a noise background using the coherent state analysis outlined above.

To illustrate how polarisation information can be combined with the coherent state analysis consider the following simulated results for the UWB radar response of a pair of spatially separated dipole wire antennas oriented at 45° as shown in figure 8. This target is chosen because the high Q wires yields an impulse response which is well matched to the Gabor wave basis. Other structures require different wavelet bases.

Figure 9 shows the radiated impulse response for this target. Notice that the HH return contains an overlayed response from both dipoles whereas the VV return contains only a response from the front dipole, the rear being orthogonally polarised. The HV signal is clearly visible from the front dipole. We can see that the polarimetric UWB response consist of the time shifted transient waveforms, with different information in each polarised channel. We can use the Gabor transform to analyse such signals. Since the coefficients C_{mn} are complex, we can then generate the generalised Huynen parameters to identify the polarimetric nature of the scattering centres [14]. Figure 10 shows the Gabor/Huynen plane for this dipole target. Figures 10 (a) and 10 (b) show the k_0 and k_1 images where.

$$k_0 = C_{mn}{}^{kk} + C_{mn}{}^{vv} \qquad k_1 = C_{mn}{}^{kk} - C_{mn}{}^{vv}$$

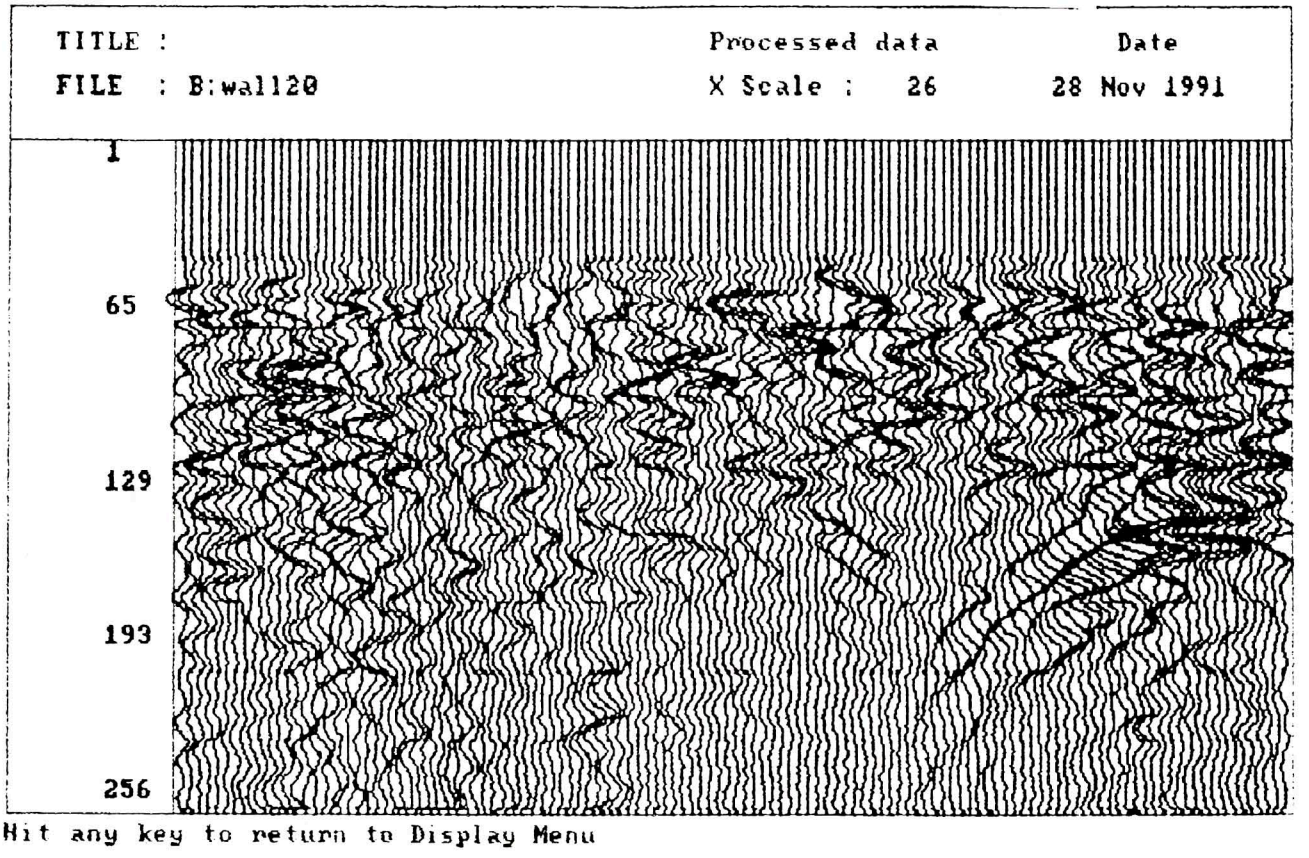

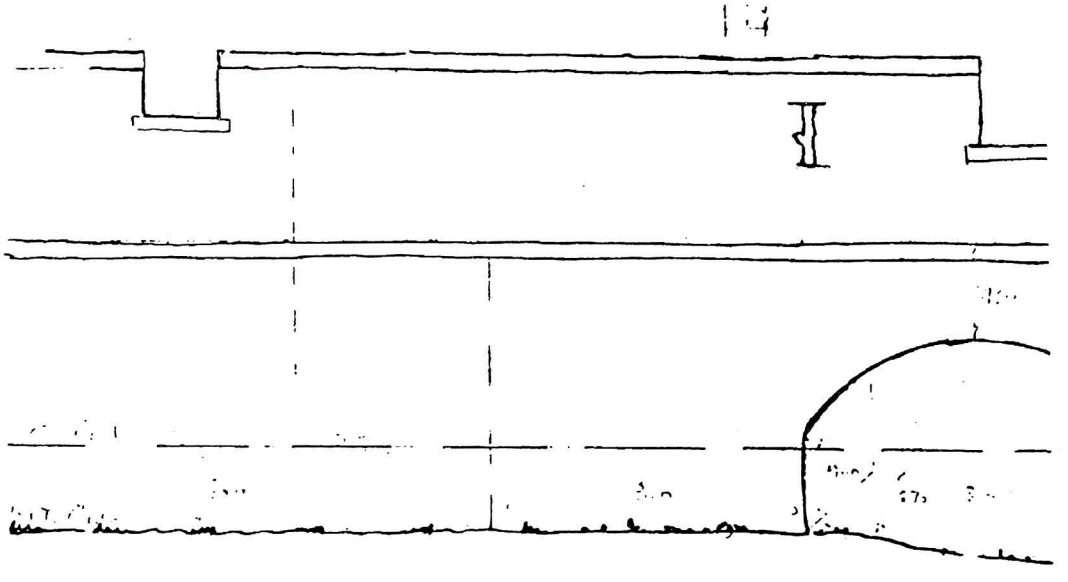

Fig. 7(a) - Copolarised GPR Image of York City Walls.

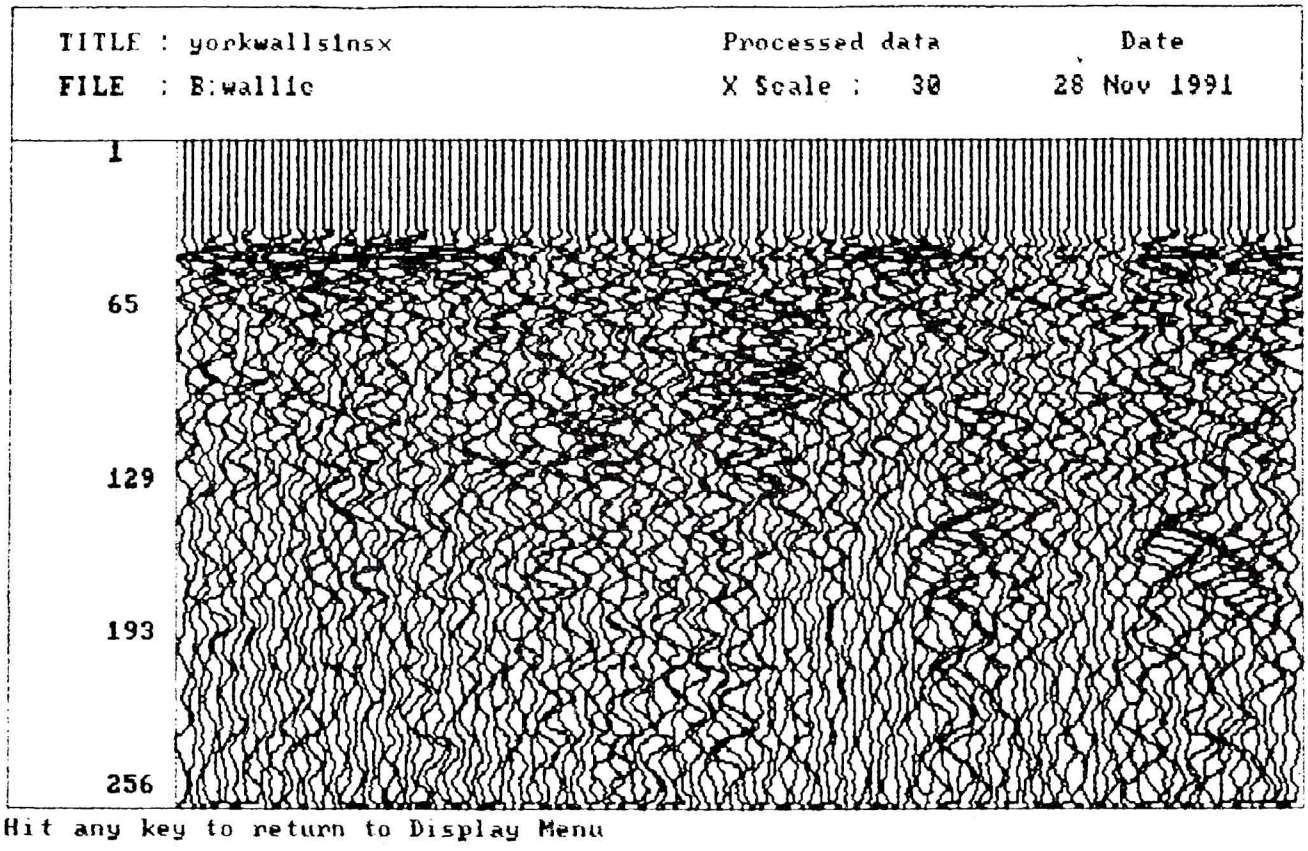

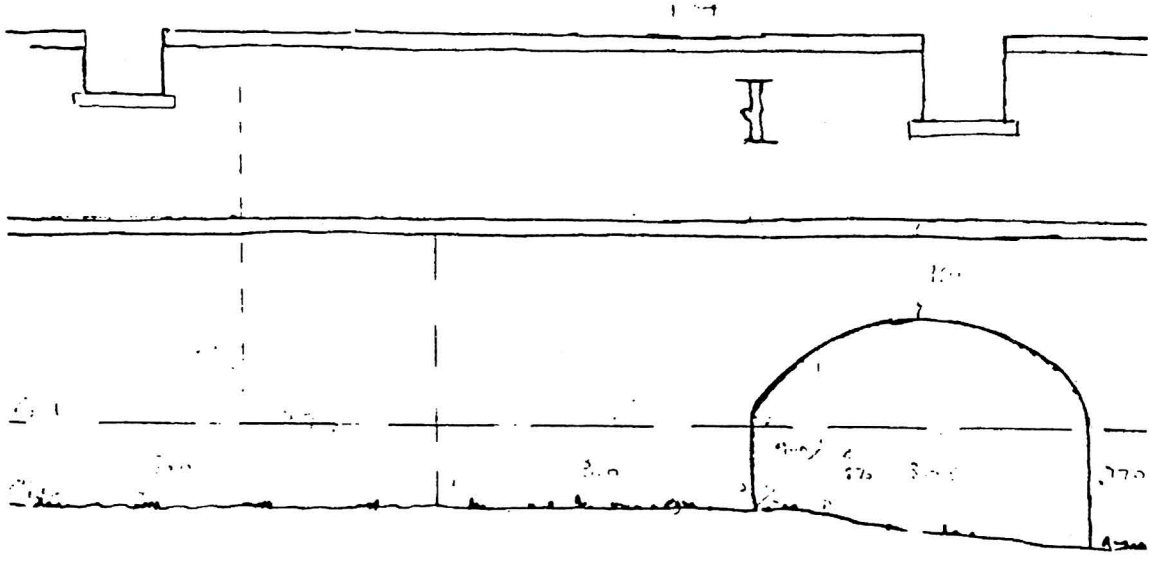

Fig. 7(b) - Cross Polarised GPR Image of York City Walls.

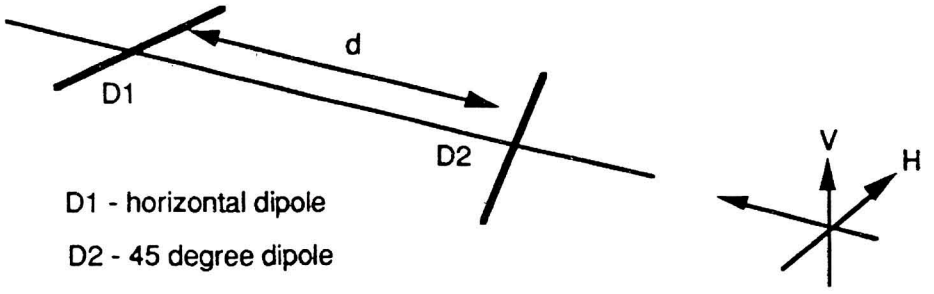

Fig. 8 - Twin Dipole Target for Polarimetric UWB Simulation.

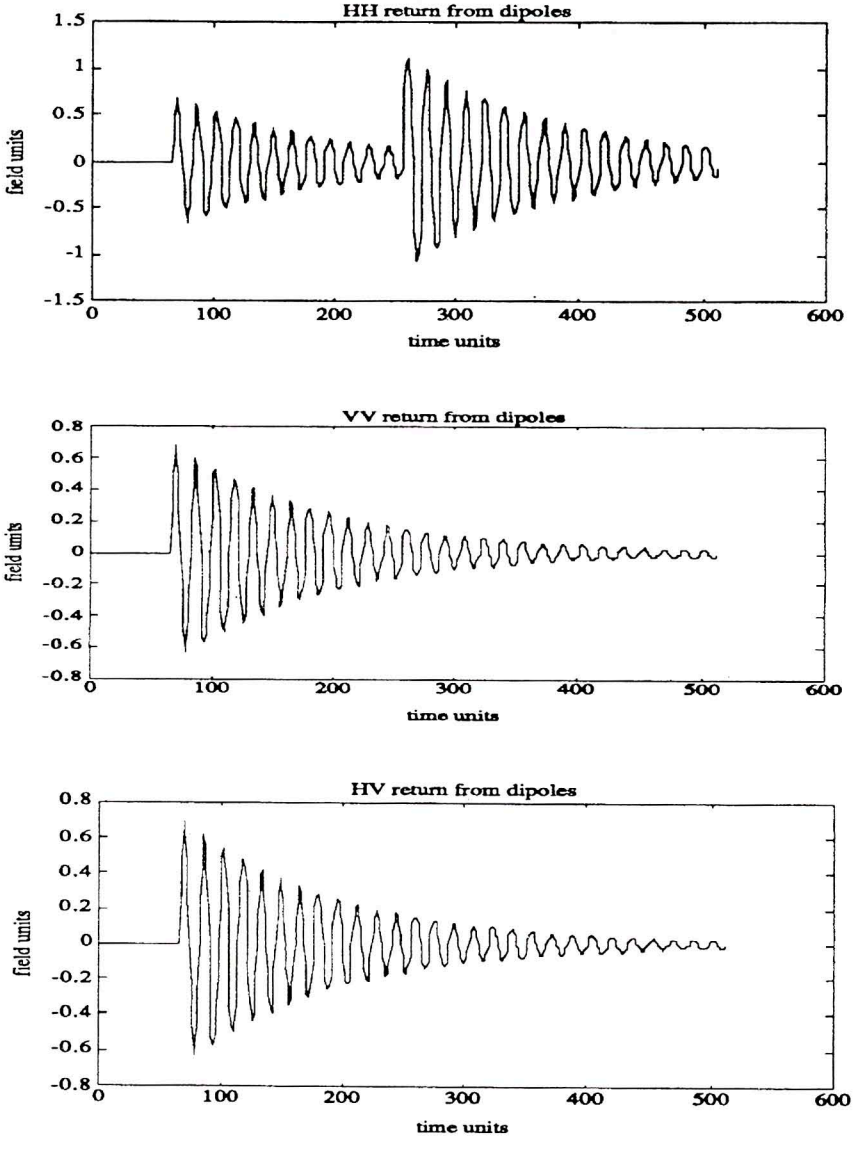

Fig. 9 - Radiated Impulse Response for Twin Dipole Target.

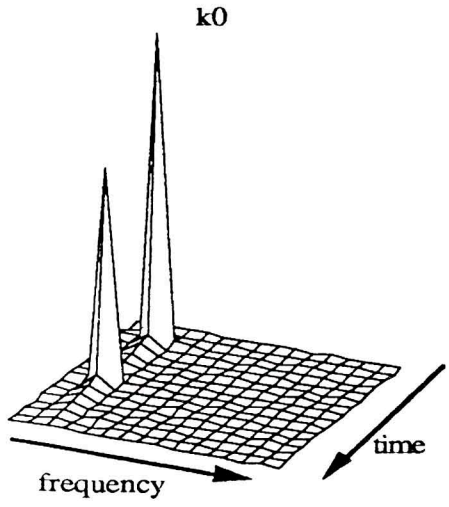

Figure 10(a)

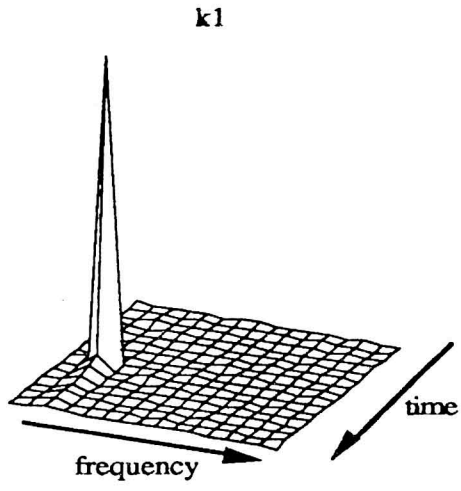

Figure 10(b)

Gabor Transform 0f C

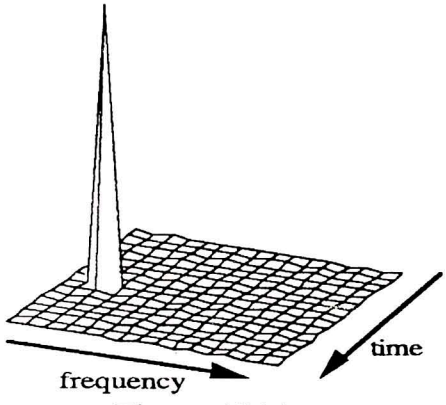

Figure 10(c)

Gabor Transform of D

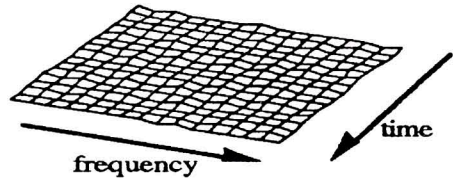

Figure 10(d)

Gabor Transform 0f E

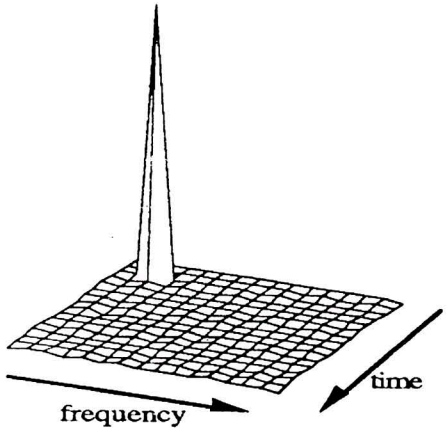

Figure 10(e)

Gabor Transform of F

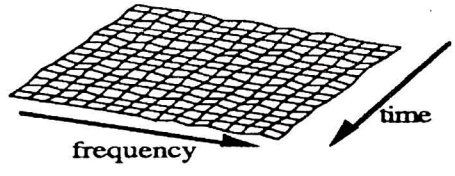

Figure 10(f)

Fig. 10 - Gabor/Huynen Plane for Twin Dipole Target.

These images show the two dipoles as point scatters (this is because the Gabor waves are well matched to the damped sinusoidal of the dipoles). By looking at the k_1 image we can see that only the rear scatterer (the horizontal dipole) has a non-symmetric target component, the nature of which we can extract from the Huynen parametres C, D, E and F. These are shown in figures 10 (c) to 10 (f). Note that the front target has a nonzero E component and zero C, D and F components, indicating that it is a linear dipole scatterer at 45°. The rear target on the other hand has three zero coefficients with only C being nonzero, indicating that it is a horizontally oriented dipole. This simple example illustrates how we can combine the coherent state analysis of time domain waveforms with the Huynen parametric description of polarimetric targets. Future work will be aimed at extending this formalism to more complicated scattering elements. Note also that the relative timing in the polarimetric signals can be used to design a multi-dimensional matched filter for such targets to enhance their detection in noise.

CONCLUSION

In this paper we have outlined some recent developments in the application of polarimetric techniques in radar imaging. We have concentrated on two main areas: the use of optimum polarisation theory in SAR imaging for remote sensing applications and the combined use of polarimetric information and coherent state analysis of ultra wide band radar signals.

In the case of optimum polarisations we have shown that great care must be used when using algorithms for the calculation of optimum states for distributed targets. We have outlined a better policy of applying the well understood single feature optimisation theory to the dominant eigenvector in a target decomposition of the distributed target. We presented processed JPL SAR images to support this idea.

In the case of UWB radar imaging, we showed how such signals can be used to extract both global and local target information. Both types of information are required in the case of non co-operative target identification where there is no a priori information of the location of scattering centres. We propose the use of dual polarisation UWB radars for the imaging of such targets and presented some initial results of polarimetric ground probing radar images of sub surface features.

We suggest that the use of coherent state analyses is promising as a general formulation of UWB radar problems. It permits the logical extension of elliptical polarisations to broad band signals and hence generalises the Huynen target parameters for use with UWB radars. We presented a simple example of imaging a high Q composite wire target and showed how the orientation of the wire targets could be extracte by using Gabor wave analysis and the Huynen parameters.

ACKNOWLEDGEMENTS

We wish to acknowledge the support of DRA Electronics Division at RSRE Malvern for the use of data from their time domain radar range on the sphere and cylinder targets. We also wish to acknowledge the support of JRC ISPRA for use of the POLTOOL software package for analysis of JPL SARA data. Finally, we would like to thank Dr P D Smith of the University of Dundee for his Mie series caculation of the sphere time domain impulse response.

REFERENCES

[1] D.L. Evans J.J. van Zyl "Polarimetric Imaging Radar: Analysis Tools and Applications", Chapter 7 in Progress in Electromagnetics Research (PIER) Volume 3, Ed. J.A. Kong, Elsevier Press, 1990.

[2] S. H. Yueh, J.A. Kong, J.K. Jao, R.T. Shin, H.A. Zebker, T. Le Toan, H. Ottl, "K-Distribution and Polarimetric Terrain Radar Clutter", Chapter 4 in Electromagnetics Research (PIER) Volume 3, Ed. J.A. Kong, Elseiver Press, 1990.

[3] A.P. Agrawal, W.M. Boerner "Redevelopment of Kennaughts Target Characteristic Polarisation State Theory Using the Polarisation Ratio Formalism for the Coherent Case", IEEE Trans GSRS Vol. 27, No. 1 pp. 2-14 January 1989

[4] S.R. Cloude "Optimisation Methods in Radar Polarimetry" Proceedings of IEE International Conference on Antennas and Propagation, ICAP 91, University of York, pp. 392-395, April 1991.

[5] J.R. Andrews "Comparison of Ultra-Fast Rise Time Sampling Oscilloscopes", Picosecond Pulse Labs Application Note AN-2a, Boulder, COlorado 80306, USA, February 1989

[6] O. Rioul, M. Vetterli "Wavelets and Signals Processing", IEEE Signal Processing magazine, October 1991, pp. 14-35

[7] J. R. Huynen "The Stokes Matrix Parameters and their Interpretation in Terms of Physical Target Properties", Recueil Des Communications des Journees Internationales de la Polarimetric Radar (JPR 90), University of Nantes, France, march 1990.

[8] W.M. Boerner "Polarisation Dependance in EM Inverse problems", IEEE Trans AP-29, pp. 262-271, March 1981.

[9] J.R. Huynen "Phenomenological Theory of Radar Targets" PhD Thesis, University of Technology, Delft, Netherlands, December 1970.

[10] S.R. Cloude, "Polarimetric Techniques in Radar Signal Processing", Microwave Journal, Vol. 26 No. 7, pp. 119-129, July 1984.

[11] E. Pottier, J. Saillard "Contribution of Radar Polarimetry to High Resolution Radar Imaging", recueil Des Communications des Journees Internationales de la Polarimetrie Radar (JIPR 90), University of nantes, France, March 1990.

[12] J.J. van Zyl H.A. Zebker "Imaging Radar Polarimetry", Chapter 5 in Electromagnetics Research (PIER) Volume 3, Ed. J.A. Kong, Elsevier Press, 1990

[13] A.B. Kostinski, B.D. James, W.M. Boerner "Optimal Reception of Partially Polarised Waves" JOSA A Volume 5, pp. 58-64, Jauary 1988.

[14] J.R. Huynen "Theory and Applications of the N-target Decomposition Theorem", Recueil Des Communications des Journees Internationaled de la Polarimetric Radar (JIPR 90), University of Nantes, France, March 1990.

[15] W.M. Boerner et al eds. Direct and Inverse methods in Radar Polarimetry, Proceedings NATO-ARW-DIMRP, Bad Windsheim, September 1988, NATO ASI Series, Series C, Maths and Phys Science, Volume 143, D Reidel Pub., Dordrecht 1992.

[16] S.R. Cloude "The Differential Coherency Matrix: a New Calculus for Modelling Propagation and Scattering in Depolarising Media", Proceedings of ESA International Workshop on Multi-Parameter Radar Applied to Microwave Propagation, Graz, Austria, Sept 1991.

[17] G.A. Ioannidis D.E. Hammers "Optimum Antenna Polarisation for Target Discrimination in Clutter", IEEE Trans AP-27, pp. 57-363, May 1979.

[18] J.A. Kong, S.H. Yueh, H.H. Lim, R.T. Shin J.J. van Zyl "Classification of Earth Terrain Using Polarimetric Synthetic Aperture Radar Images", Chapter 6 in Progress in Electromagnetics Research (PIER) Volume 3, Ed. J.A. Kong, Elsevier Press, 1990.

[19] S.R. Cloude "Polarimetric Optimisation based on the Target Covariance Matrix", Electronics Letters, Vol. 26 No 20 September 1990, pp. 1670-1671.

[20] S.R. Cloude "The Application of Group Theory to Radar Polarimetry", Proceedings of International Conference on EM in Aerospace Applications, ICEAA 91, Torino, Italy, pp. 295-298, Sept 1991.

[21] Proceedings of Conference on Ultra Wide Band Radar, SPIE Proceedings Volume 1631, Los Angeles, January 1992.

[22] M. Born E Wolf "Principles of Optics", Chapter 10, Pergamon Press, New York 1964.

[23] E.M. Kennaugh, D. Moffat "Transient and Impulse Response Approximations", Proc IEEE Vol. 53, pp. 893-901, 1965.

[24] I. Daubechies "Orthogonal Bases of Compactly Supported Wavelets", Comm. on Pure and Applied Math. Vol. 41, No. 7, pp. 909-996 (1988).

[25] B.B. Wells "Applications of Wavelets in Radar", Proceedings of PIERS Symposium, Boston, July 1991, p. 653.

[26] I. Daubechies "The Wavelet Transform: Time Frequency Localisation and Signal Analysis", IEEE Trans IT-36, No. 5, pp. 961-1005 Sept. 1990.

[27] B. Friedlander, B. Porat "Detection of Transient Signals by the Gabor Representation", IEEE Trans ASSP-37, pp. 169-179, 1989.